See ARTICLE page 1118

Epigenetic control of Foxp3 by SMYD3 H3K4 histone methyltransferase controls iTreg development and regulates pathogenic T-cell responses during pulmonary viral infection

DE de Almeida Nagata[1], H-A Ting[1], KA Cavassani[1], MA Schaller[1], S Mukherjee[1], C Ptaschinski[1], SL Kunkel[1] and NW Lukacs[1]

The generation of regulatory T (Treg) cells is driven by Foxp3 and is responsible for dampening inflammation and reducing autoimmunity. In this study, the epigenetic regulation of inducible Treg (iTreg) cells was examined and an H3K4 histone methyltransferase, SMYD3 (SET and MYND Domain 3), which regulates the expression of Foxp3 by a TGFβ1/Smad3 (transforming growth factor-β1/Smad3)-dependent mechanism, was identified. Using chromatin immunoprecipitation assays, SMYD3 depletion led to a reduction in H3K4me3 in the promoter region and CNS1 (conserved noncoding DNA sequence) of the *foxp3* locus. SMYD3 abrogation affected iTreg cell formation while allowing dysregulated interleukin-17 production. In a mouse model of respiratory syncytial virus (RSV) infection, a model in which iTreg cells have a critical role in regulating lung pathogenesis, SMYD3$^{-/-}$ mice demonstrated exacerbation of RSV-induced disease related to enhanced proinflammatory responses and worsened pathogenesis within the lung. Our data highlight a novel activation role for the TGFβ-inducible SMYD3 in regulating iTreg cell formation leading to increased severity of virus-related disease.

INTRODUCTION

Epigenetic regulation of gene activation is organization of the loci into transcriptionally active or silent states altering the accessibility of transcription factors and polymerases to gene promoters and enhancers.[1,2] Histone modifications that regulate chromatin accessibility include methylation, acetylation, ubiquitination, phosphorylation, and so on, and determine the transcriptional status of the gene loci by exposing or sequestering the promoter region.[3] Methylation of lysines on histone H3 for the regulation of chromatin accessibility, especially H3K4 trimethylation, is associated with transcriptional activation. This activation mark is offset by methylation of H3K9 and H3K27, associated with transcriptional silencing of the gene. The modifications rely on both methyltransferases that add and demethylases that remove methyl groups from specific lysines allowing plasticity to gene activation.[4] Thus, the specific regulation of genes by chromatin modifications is likely both gene and cell specific.

The SET and MYND Domain (SMYD) are a family of SET histone methyltransferases involved in chromatin regulation and gene transcription.[5] SMYD3 was previously identified as an H3K4me3 histone methyltransferase that may be a proto-oncogene based on its expression in numerous cancers and because of a cellular function observed in overexpression studies of normal cells or in silencing studies in tumors.[6–8] SMYD3 is a regulator of matrix metallopeptidase 9-modifying H3K4me3 marks on the matrix metallopeptidase 9 promoter and affecting tumor invasiveness.[9] The function and regulation of SMYD3 in nontransformed cells or its regulation in immune cells has not been examined.

The differentiation of mature T cells into different phenotypes is controlled by multiple cytokines and related transcription

[1]Department of Pathology, University of Michigan Medical School, Ann Arbor, Michigan, USA. Correspondence: NW Lukacs (nlukacs@umich.edu)

Received 9 September 2014; accepted 2 January 2015; published online 11 February 2015. doi:10.1038/mi.2015.4

factors that allow the immune system to 'fine-tune' responses to pathogen insult.[10,11] An important T-cell phenotype is the Foxp3-expressing regulatory T (Treg) cell that can affect the other T helper phenotypes and their accompanying responses.[12] The central determinant of Treg development is Foxp3 expression, a transcription factor that is constitutively expressed in thymus-derived naturally occurring Treg (nTreg) cells and upregulated in inducible Treg (iTreg) cells.[13,14] Also important in the generation of iTreg cells is the activation of TGFβ/Smad3 (transforming growth factor-β/Smad3) signaling pathway,[15] which correlates with the alteration of a conserved noncoding DNA sequence (CNS1) element at the *foxp3* locus and regulates Foxp3 expression in iTreg cells.[16–18] The present studies expand our knowledge of epigenetic regulation during the development of Treg cells.[10]

In the present study, *SMYD3* was identified as a TGFβ/Smad3-associated primary epigenetic mediator of Foxp3 in iTreg cells, while it also regulates interleukin-17 (IL-17) production. *In vitro* silencing or CD4-specific genetic deficiency of TGFβ-inducible SMYD3 reduces iTreg cell development and *in vivo* leads to exacerbated virus-induced lung pathology associated with dysregulated proinflammatory cytokine production. Overall, these data highlight a novel activation role for SMYD3 methyltransferase in the regulation of Foxp3 expression, generation of iTreg cells, and modulation of proinflammatory cytokine production.

RESULTS

TGFβ induces SMYD3, an H3K4 methyltransferase, in iTreg-differentiating cells

The present studies focused on examining the overall epigenetic regulation in iTreg cells by initiating an unbiased examination of epigenetic enzymes using a gene subset array during iTreg cell development. After 48 h of iTreg-skewing conditions, mRNA analysis of chromatin remodeling enzymes was performed. The data in **Figure 1a** depict the methyltransferases analyzed and show the only gene that was significantly upregulated during the iTreg-skewing process, SMYD3 (H3K4 methyltransferase). Subsequent studies using quantitative real-time PCR (q-RT-PCR) analysis of *SMYD3* mRNA levels in naïve $CD4^+$ T cells under iTreg-skewing conditions *in vitro* showed a continuous increase in the gene expression levels over a period of 120 h (**Figure 1b**). Also, the sustained expression of *smyd3* required the continuous presence of TGFβ in culture as expression levels diminished once TGFβ was removed (**Figure 1b**). When analyzing the SMYD3 chromatin-modifying mark H3K4me3 after 3 days under skewing conditions, results showed that iTreg cells had a significant increase in H3K4me3 expression compared with TH0 cells (**Figure 1c**). By stimulating naïve $CD4^+$ T cells with each component of the iTreg cell differentiation individually, our data demonstrated that TGFβ is a primary inducer of SMYD3 (**Supplementary Figure 1A** online). Moreover, using naïve $CD4^+$ T cells derived from mice (**Supplementary Figure 1B**) and from human peripheral blood mononuclear cells (**Supplementary Figure 1C**), TGFβ-induced SMYD3 protein level was dose dependent, as indicated by western blot and by q-RT-PCR analyses. Next, to verify whether SMYD3 was upregulated in all cells exposed to TGFβ or only in converted $Foxp3^+$ iTreg cells, naïve T cells were isolated from $Foxp3^{egfp}$ mice and skewed toward iTreg cells. Converted iTreg cells ($CD4^+CD25^+Foxp3^{egfp+}$) and nonconverted effector T cells ($CD4^+CD25^+Foxp3^{egfp-}$) were FACS- (fluorescence-activated cell sorting) sorted. As shown in **Figure 1d**, *smyd3* was overexpressed in converted $Foxp3^{egfp+}$ iTreg cells but not in nonconverted $Foxp3^{egfp-}$ effector T cells, indicating that SMYD3 is correlated with the expression of Foxp3. To verify the effect of TGFβ on SMYD3 protein induction in iTreg cells and its colocalization in the nucleus, both naïve $CD4^+$ T cells and 4-day skewed iTreg cells were assessed using a SMYD3-specific antibody and confocal microscopy. The cells under iTreg-skewing conditions, but not naïve T cells, had SMYD3 protein expressed in the nucleus (**Figure 1e**). Next, to further confirm the correlation of SMYD3 with Foxp3 expression, using murine and human naïve $CD4^+$ T cells skewed towards iTreg cells *in vitro*, it was verified that *smyd3* expression paralleled the expression of *foxp3*. Both mRNA levels of *foxp3* and *smyd3* were upregulated in iTreg-skewing cells in mouse and human cells (**Figure 1f**). Also, Foxp3 and SMYD3 protein levels were checked in both TH0 and iTreg cells and showed higher SMYD3 and Foxp3 protein levels in iTreg cells (**Supplementary Figure 1D**). Thus, these results suggest that the epigenetic enzyme SMYD3 is specifically induced by TGFβ and coordinated with Foxp3 expression in iTreg cells.

SMYD3 correlates with Foxp3 expression only in iTreg cells but not in nTreg cells

We also characterized the expression of SMYD3 in nTreg cells by isolating thymic nTreg cells ($CD4^+CD25^+Foxp3^{egfp+}$) or naïve ($CD4^+CD25^-Foxp3^{egfp-}$) T cells from $Foxp3^{egfp}$ mice. Although Foxp3 expression was high, the expression level of SMYD3 in thymic-derived nTreg cells was low compared with naïve cells (**Figure 2a**), suggesting that SMYD3 correlates with Foxp3 only in iTreg cells but not in nTreg cells. To determine whether SMYD3 would affect Foxp3 expression in nTreg cells, thymic nTreg ($CD4^+CD25^+Foxp3^{egfp+}$) cells from $Foxp3^{egfp}$ mice were isolated and transfected with control or *SMYD3* small interfering RNA (siRNA). The results show that SMYD3 knockdown did not affect Foxp3 expression in nTreg cells compared with control siRNA (**Figure 2b**).

To further determine the possible role of SMYD3 in the regulation of Foxp3 in nTreg cells *in vivo*, we conditionally deleted *SMYD3* in $CD4^+$ T cells by crossing novel $SMYD3^{fl/fl}$ mice generated by our lab with $CD4^{Cre}$ mice. Therefore, resultant mice (hereafter referred as $SMYD3^{-/-}$) are SMYD3 deficient in all mature CD4+ T cells, as well as in CD8+ and CD4+CD8+ T cells. All animals were viable, healthy, and fertile. $SMYD3^{-/-}$ mice had reduced number of thymic $CD4^+CD25^+Foxp3^+$ nTreg cells compared with wild-type (WT) mice (**Figure 2c**). However, despite the reduced numbers of nTreg cells, all $SMYD3^{-/-}$ mice were born at normal Mendelian ratios and displayed neither phenotypic alteration nor autoimmunity with no signs of weight loss,

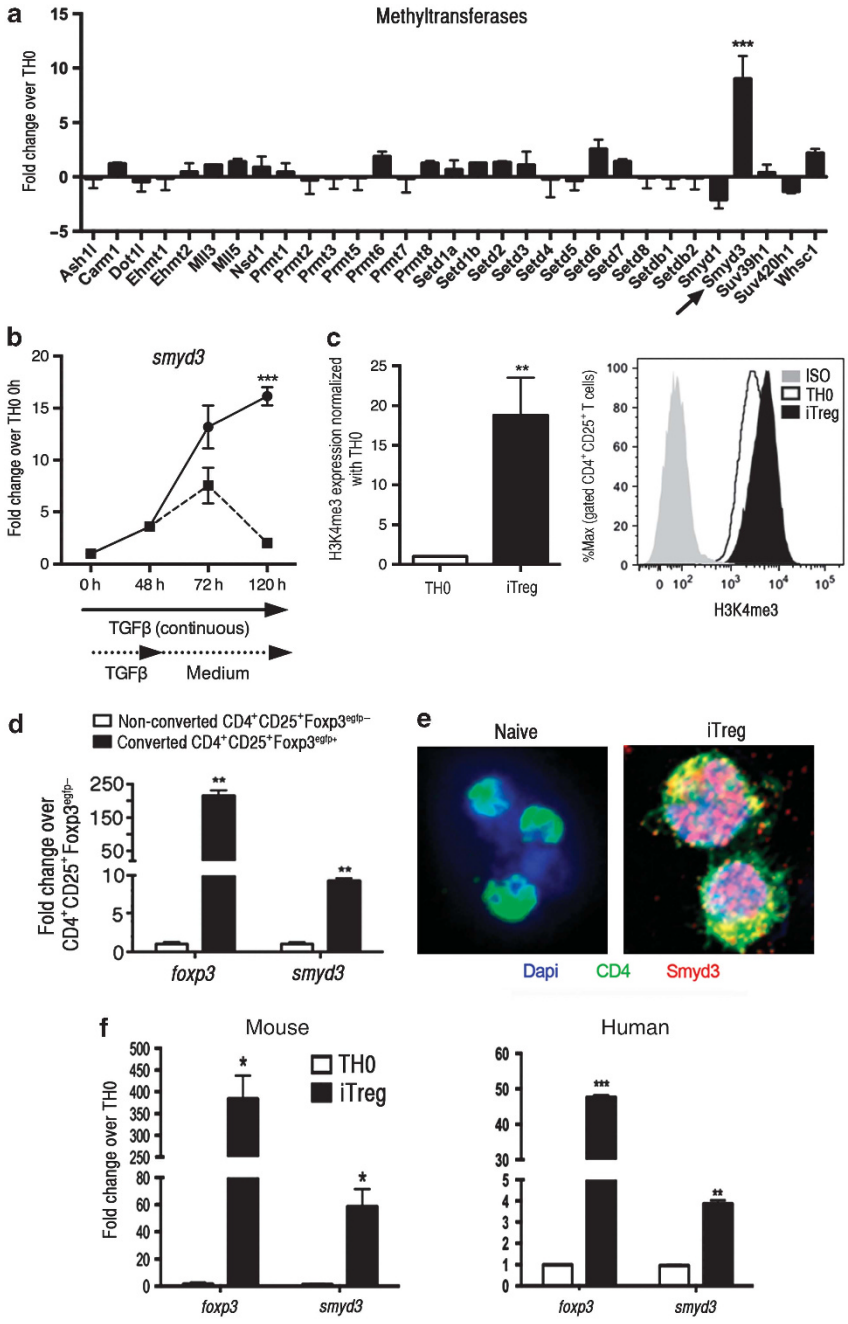

Figure 1 Transforming growth factor-β1 (TGFβ1) regulates the expression of SMYD3 in inducible regulatory T (Treg) cells. (**a**) Naïve T cells were cultured under TH0 or skewed towards inducible Treg (iTreg) cells. After 48 h, the levels of methyltransferases were each assessed by PCR arrays. Data are representative of three independent experiments. (**b**) *SMYD3* expression was assessed by quantitative real-time PCR (q-RT-PCR) in naïve T cells skewed under iTreg conditions over 120 h. At 48 h, some wells had TGFβ1 withdrawn from the culture, mRNA extracted, and gene expression of *SMYD3* assessed. (**c**) Bar graph shows expression of H3K4me3 in iTreg cells normalized with TH0 and histogram showd H3K4me3 expression in gated CD4 + CD25 + T cells in iTreg and TH0 cells at 3 days of differentiation. (**d**) Naïve CD4$^+$ T cells from Foxp3^{egfp} mice were skewed towards iTreg cells. Converted CD4$^+$CD25$^+$Foxp3^{egfp+} iTreg cells and CD4$^+$CD25$^+$Foxp3^{egfp-} effector cells were FACS- (fluorescence-activated cell sorting) sorted from 5-day cultures and mRNA was extracted with Foxp3 and *SMYD3* expression was then analyzed by q-RT-PCR. (**e**) Naïve CD4$^+$T cells and iTreg cells were stained with anti-CD4 and anti-SMYD3 and evaluated by confocal microscopy (1000X). (**f**) Naïve CD4$^+$T cells were isolated from mouse spleens and human peripheral blood mononuclear cells, activated under TH0 or iTreg-skewing condition for 5 days, mRNA extracted, and gene expression of Foxp3 and SMYD3 assessed. Data are means ± s.e. (standard error) of triplicate samples and are representative of at least two independent experiments. *$P<0.05$, **$P<0.01$, and ***$P<0.001$.

lymphadenopathy, or splenomegaly, further suggesting that nTreg cells may not be substantially regulated by SMYD3 when using the CD4-Cre-targeted mice. Furthermore, histological sections of key tissues from SMYD3$^{-/-}$ showed no pathological alterations at age 8 weeks or 6 months (**Supplementary Figure 3A**). To assess whether SMYD3

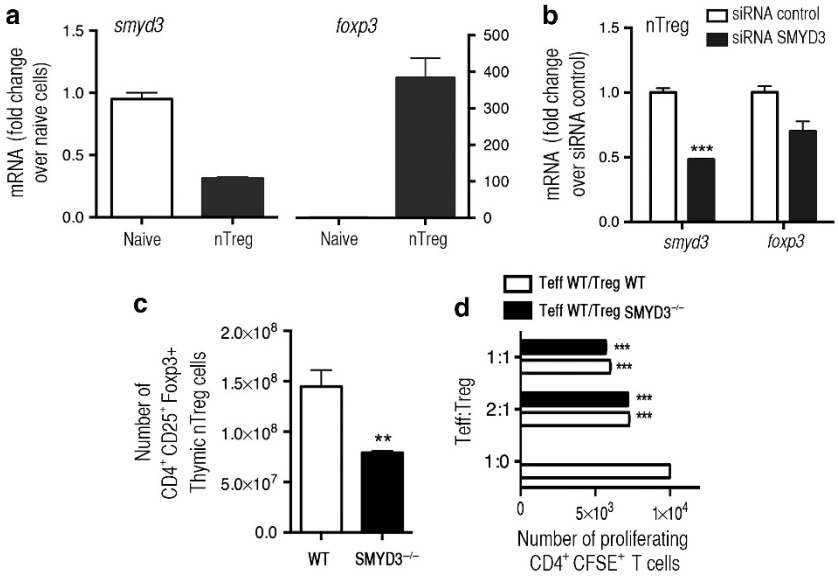

Figure 2 Transforming growth factor-β (TGFβ)-inducible SMYD3 correlates with Foxp3 expression in inducible but not in natural regulatory T (nTreg) cells. (**a**) $CD4^+CD25^+Foxp3^{egfp+}$ nTreg cells and $CD4^+CD25^-Foxp3^{egfp-}$ T cells were isolated from the thymus of $Foxp3^{egfp}$ mice. *Smyd3* and *foxp3* mRNA expression was analyzed by quantitative real-time PCR (q-RT-PCR). (**b**) nTreg cells were isolated as in **a** and transfected with SMYD3 or control small interfering RNA (siRNA). After 24 h, *smyd3* and *foxp3* expression was analyzed. (**c**) Flow cytometric analysis of $CD4^+CD25^+Foxp3^+$ nTreg cells in the thymus of $SMYD3^{-/-}$ and wild-type (WT) mice. (**d**) Treg suppression assay comparing suppressive function of nTreg cells derived from WT and $SMYD3^{-/-}$ mice cocultured with carboxyfluorescein succinimidyl ester (CFSE)-labeled WT naïve $CD4^+$ T cells stimulated with anti-CD3 and anti-CD28. Data are representative of three independent experiments and show means ± s.e.m. of four replicates. $^*P<0.05$, $^{**}P<0.01$, and $^{***}P<0.001$.

was regulating the suppressive function of nTreg cells, a suppression assay was performed using WT and $SMYD3^{-/-}$ FACS-sorted $CD4^+CD25^{HI}$ cells ($Foxp3^+$ nTreg cells; >95% purity) isolated from naïve mice. Our data show that both WT- and $SMYD3^{-/-}$-derived nTreg cells were able to suppress the proliferation of carboxyfluorescein succinimidyl ester (CFSE)-labeled $CD4^+$ T effector cells when cultured at Teff:Treg ratio of 2:1 or 1:1, suggesting that the $Foxp3^+$ nTreg cells generated by the $SMYD3^{-/-}$ mice have no defect in their suppressive function (**Figure 2d**). Thus, our results indicate that SMYD3 is not required for Foxp3 expression in nTreg cells and do not alter their suppressive function.

The induction of SMYD3 in iTreg cells is mediated by a Smad-dependent mechanism

As our data in **Figure 1** indicated that TGFβ was a primary inducer of SMYD3, we interrogated the *SMYD3* promoter gene for Smad binding element (5′-GTCTG-3′).[19] Three Smad binding elements were identified within 1.1 kb of the *SMYD3* promoter region (**Figure 3a**), with one Smad binding element that is evolutionarily conserved within the minimal *SMYD3* promoter (−104 bp from TSS) (**Figure 3b**). Using chromatin immunoprecipitation (ChIP) assay, iTreg cells showed enhanced Smad3 at the SMYD3 promoter region when compared with TH0 cells (**Figure 3c**). When SiS3, a Smad3 inhibitor, was used in iTreg-skewing cell cultures, it inhibited the expression of SMYD3 (**Figure 3d**). Compared with a control siRNA, Smad3 siRNA-transfected iTreg cells displayed significant decreases in SMYD3 as well as its chromatin mark H3K4me3 by the western blot analysis (**Figure 3e**). The downregulation of SMYD3 was accompanied by decreased Foxp3 protein using flow cytometry (**Figure 3f**), in agreement with previous studies reporting the role of TGFβ/Smad3 signaling pathway for iTreg conversion.[15] The data show that *SMYD3* expression and H3K4 trimethylation are reduced in the absence of Smad3 signaling.

SMYD3 depletion inhibits Foxp3 expression during iTreg cell development

To determine whether SMYD3 was involved in iTreg development, an siRNA knockdown approach was used. Compared with control siRNA, SMYD3 siRNA significantly reduced the *smyd3* mRNA expression in splenic-naïve $CD4^+$ T cells 24 h after transfection (**Figure 4a**). Examination of the SMYD3 knockdown effect in iTreg cell conversion, assessed by *smyd3* and *foxp3*, demonstrated that in the SMYD3 siRNA-transfected naïve $CD4^+$ T cells, there was an abrogation of iTreg cell development by q-RT-PCR (**Figure 4b**) and flow cytometry (**Figure 4c**), suggesting that SMYD3 regulates iTreg cell conversion. Importantly, inhibition of SMYD3 had no effect on apoptosis (**Supplementary Figure 2A**) or the proliferative capacity of TH0 or iTreg cells (**Supplementary Figure 2B**), suggesting that the absence of SMYD3 did not alter cell survival or proliferation. The effect of SMYD3 on Foxp3 stability was investigated by transfecting iTreg cells differentiated *in vitro* with SMYD3 or control siRNA. Silencing *SMYD3* in differentiated iTreg cells resulted in decreased *foxp3*

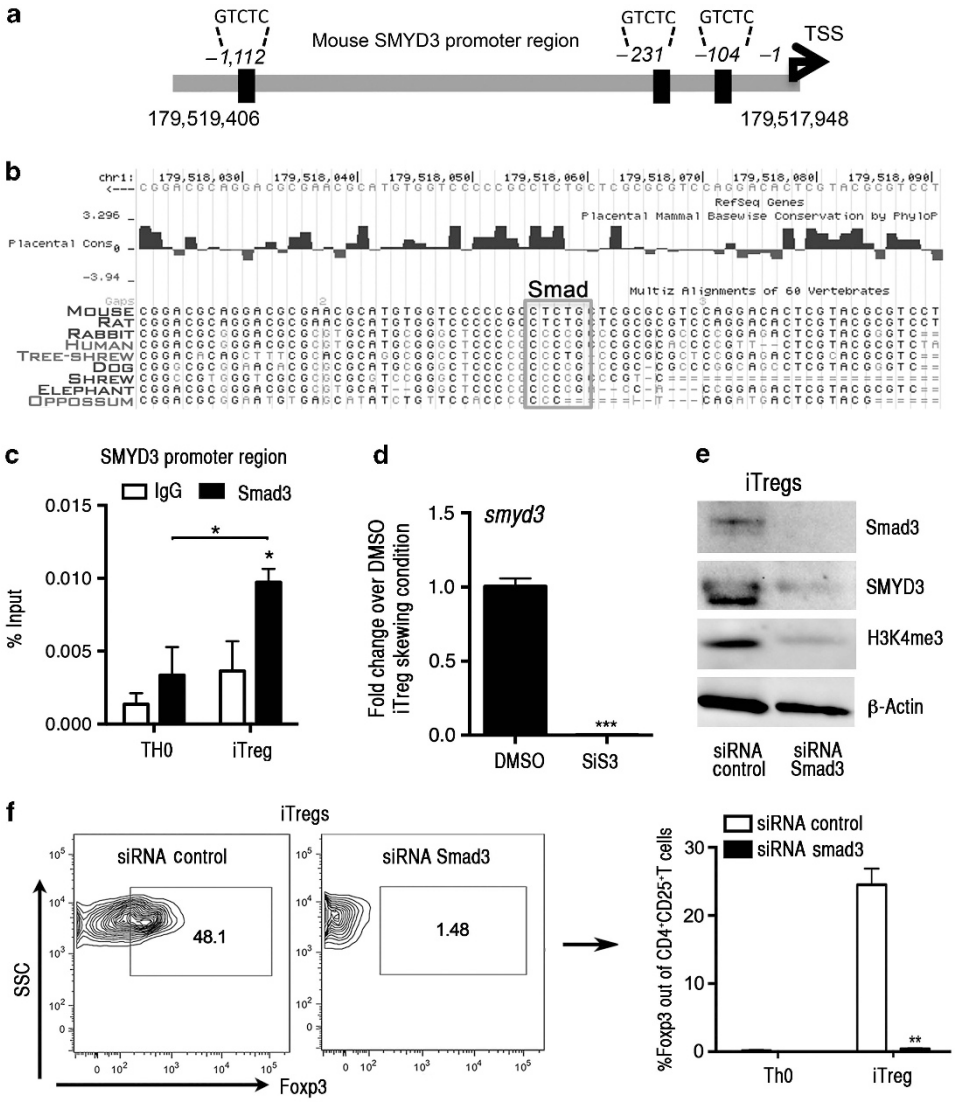

Figure 3 The induction of SMYD3 in inducible regulatory T (iTreg) cells is mediated in a Smad3-dependent manner. (**a**) Schematic of the murine SMYD3 promoter region (accession no. NM_027188) highlighting potential putative Smad3 binding sites at −104, −231, and −1112 bp upstream of the SMYD3 transcription starting site. (**b**) A Smad3 binding site is evolutionarily conserved within the minimal *SMYD3* promoter (104 bp). Conserved Smad3 binding site on *SMYD3* promoter extracted from USCS Genome browser on Mouse (GRCm38/mm10) Assembly. (**c**) Cells were cultured in complete RPMI under TH0 or iTreg cell-skewing conditions for 18 h. Chromatin immunoprecipitation (ChIP)-quantitative PCR was performed in the *SMYD3* promoter site using Smad3 antibody or species-matched immunoglobulin G (IgG) as control. Data show four replicates and are representative of three independent experiments (*$P<0.05$). (**d**) Naïve $CD4^+$ T cells were isolated and stimulated under iTreg differentiation conditions in the presence of the Smad3 inhibitor SiS3 (10 μm) or dimethyl sulfoxide (DMSO) for 4 days and assessed for SMYD3. (**e**) Western blots of Smad3, SMYD3, H3K4me3, and β-actin from Smad3- or control small interfering RNA (siRNA)-transfected T cells under iTreg cell-skewing conditions. (**f**) Foxp3 protein levels in naïve $CD4^+$ T cells transfected with Smad3 or control siRNA under iTreg-skewing condition. Data are means ± s.e. (standard error) and are representative of three independent experiments. *$P<0.05$, **$P<0.01$, and ***$P<0.001$. SSC, side scatter.

expression when compared with control siRNA (**Supplementary Figure 2C**), suggesting that SMYD3 has a role in the stability of Foxp3 in iTreg cells.

To examine physiological relevance of SMYD3 in iTreg cells *in vivo*, we used $SMYD3^{fl/fl}$ mice. Q-RT-PCR of *smyd3* in T cells derived from the thymus and spleens of $SMYD3^{-/-}$ compared with WT mice showed that the expression of *smyd3* was inhibited in $SMYD3^{-/-}$ mice (**Figure 4d**). Importantly, the frequency and numbers of naïve and activated/memory $CD4^+$ and $CD8^+$ T cells in $SMYD3^{-/-}$ were equivalent to WT mice (**Supplementary Figure 3B**). To characterize the effect of SMYD3 depletion in iTreg cell conversion, naïve $CD4^+$ T cells were isolated from WT and $SMYD3^{-/-}$ mice and differentiated into iTreg cells *in vitro*. $SMYD3^{-/-}$-derived and -skewed iTreg cells had a significant reduction in the expression of *smyd3* and *foxp3* compared with those from WT mice (**Figure 4e**). This latter finding was verified using flow cytometry of 5-day-skewed cell cultures demonstrating that $SMYD3^{-/-}$ mice generated decreased numbers of $CD4^+CD25^+Foxp3^+$ iTreg cells compared with WT mice

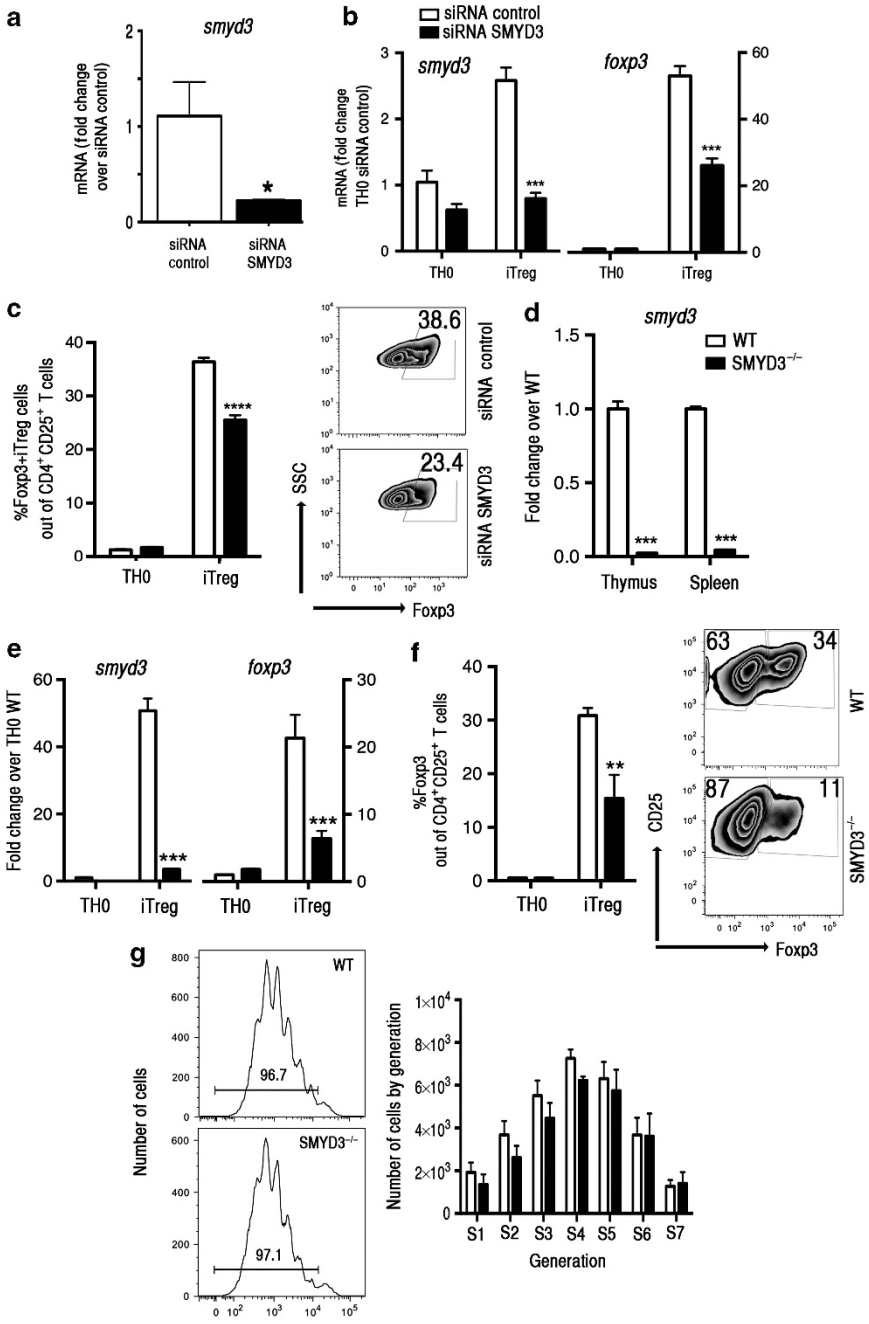

Figure 4 SMYD3 depletion inhibits Foxp3 expression during regulatory T (Treg) cell development. (**a**) Naïve CD4$^+$ T cells, transfected with SMYD3 or control small interfering RNA (siRNA), were assessed for *smyd3* expression. (**b**) After 5 days, expression levels of *smyd3* and *foxp3* were assessed in transfected cells under TH0- or inducible Treg (iTreg)-skewing conditions. (**c**) Bar graphs and zebra plots showing Foxp3 expression in gated CD4$^+$CD25$^+$ T cells. Data are presented as the mean of four wells and are representative of four independent experiments. (**d**) Expression levels of *smyd3* mRNA in CD4$^+$ T cells derived from the thymus and spleens of wild-type (WT) and SMYD3$^{-/-}$ mice. (**e**) Expression levels of *smyd3* and *foxp3* mRNA in naïve CD4$^+$ T cells from WT (white) and SMYD3$^{-/-}$ (black) differentiated under TH0- and iTreg-skewing conditions for 3 days. (**f**) Bar graphs of CD4$^+$CD25$^+$ T cells from WT (white) and SMYD3$^{-/-}$ mice (black) and zebra plots showing Foxp3 expression in gated CD4$^+$CD25$^+$ T cells skewed as in **e**. (**g**) Carboxyfluorescein succinimidyl ester (CFSE)-labeled naïve CD4$^+$ T cells derived from WT and SMYD3$^{-/-}$ mice under iTreg-skewing conditions were assessed by flow cytometry. Histogram plots show proliferation and bar graph shows the number of proliferating cells by generation at day 4. Data are representative of four independent experiments performed with $n = 3$ per group and show means ± s.e.m. of four replicates. *$P < 0.05$, **$P < 0.01$, ***$P < 0.001$, and ****$P < 0.005$.

(**Figure 4f**). Importantly, SMYD3 deletion did not modify proliferative competence of naïve CD4$^+$ T cells derived from SMYD3$^{-/-}$ mice stimulated with anti-CD3/CD28 (**Figure 4g**). These results offer genetic evidence of the functional relevance of SMYD3 in the development of TGFβ-inducible iTreg cells.

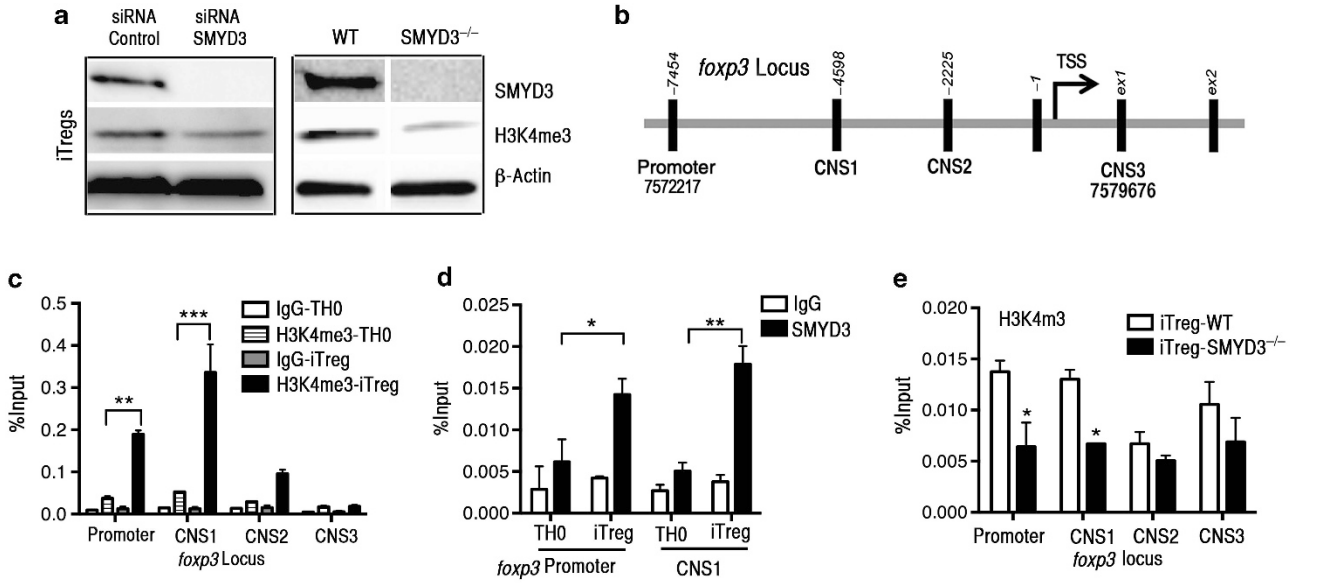

Figure 5 SMYD3 is partially responsible for H3K4 trimethylation at the *foxp3* locus in inducible regulatory T (iTreg) cells. (**a**) Western blots of SMYD3, H3K4me3, and β-actin from lysates of control or SMYD3 small interfering RNA (siRNA)-transfected wild-type (WT) naïve $CD4^+$ T cells and from WT and $SMYD3^{-/-}$-derived naïve $CD4^+$ T cells, 4 days under iTreg-differentiating conditions. (**b**) Schematic of the murine *foxp3* locus highlighting the regions investigated. Chromatin immunoprecipitation (ChIP) assays were performed in the *foxp3* promoter site, CNS1, -2, and -3 of the *foxp3* locus using H3K4me3 antibody or immunoglobulin G (IgG) as control (**c**), and in the *foxp3* promoter site and CNS1 using SMYD3 antibody or IgG as control (**d**). (**e**) ChIP assays were performed in the *foxp3* locus using H3K4me3 antibody or IgG as control or skewed T cells. Data show mean ± s.e.m. of four replicate wells and are representative of three independent experiments. $^*P<0.05$, $^{**}P<0.01$, and $^{***}P<0.001$. CNS, conserved noncoding DNA sequence.

H3K4 trimethylation ChIP of Foxp3 in iTreg cells is partially regulated by SMYD3

To further characterize SMYD3 function, we investigated whether SMYD3 depletion affects the H3K4 trimethylation in iTreg cells. Western blot analysis of naïve $CD4^+$ T cells transfected with SMYD3 siRNA or control siRNA and of naïve $CD4^+$ T cells derived from $SMYD3^{-/-}$ or WT mice under iTreg-skewing conditions shows that by either knocking down or genetically depleting *SMYD3*, the expression of H3K4me3 in iTreg-skewed cells was significantly reduced (**Figure 5a**). Transcription of the *foxp3* gene is regulated by the promoter region and also by CNS elements. CNS1, -2, and -3 encode essential information defining composition and stability of the Treg population.[16] Using ChIP analysis of H3K4 trimethylation, we specifically examined the promoter site and CNS1, -2, and 3 of the *foxp3* locus in cells from WT mice (**Figure 5b**). Compared with TH0 cells, it was found that iTreg cells have enhanced H3K4 trimethylation at the promoter site and CNS1 (**Figure 5c**). To verify that SMYD3 was the methyltransferase responsible for the modification in H3K4 in the promoter region and CNS1 of *foxp3*, we performed a ChIP assay of *SMYD3*. The results showed significant enhancement of *SMYD3* in these regions in iTreg cells (**Figure 5d**). Finally, to confirm that SMYD3 was the enzyme responsible for modifying H3K4me3 at the promoter and CNS1, $SMYD3^{-/-}$- and WT-derived iTreg-skewed cells were examined. The results showed a significant reduction in the H3K4 trimethylation levels at the promoter and CNS1 sites, but not in CNS2 and -3, of *foxp3* locus from $SMYD3^{-/-}$ mice (**Figure 5e**). Although our results indicate that SMYD3 is not the sole factor regulating Foxp3, the TGFβ-inducible SMYD3 enhances to the trimethylated state of H3K4 in specific regions of the *foxp3* locus, namely the promoter and the CNS1 element, thus facilitating gene transcription.

SMYD3-depleted $CD4^+$ T cells are poised to produce IL-17

Given that the overall T-cell proportions between $SMYD3^{-/-}$ and WT mice were similar (**Supplementary Figure 3B**), we explored the phenotypic consequences of SMYD3 ablation and Foxp3 inhibition in iTreg-developing cells. $CD4^+$ T cells were isolated from WT and $SMYD3^{-/-}$ mice and show that the baseline levels of Foxp3 expression were significantly decreased in $CD4^+$ T cells derived from $SMYD3^{-/-}$ mice (**Figure 6a**). Moreover, because Foxp3 protein prevents iTreg cell deviation to a effector cell lineage,[20] we determined if iTreg-skewed $SMYD3^{-/-}$ $CD4^+$ T cells would exhibit differences in their production of proinflammatory cytokines. Indeed, the production of IL-17 was enhanced in the supernatants derived from iTreg-skewed $SMYD3^{-/-}$ T-cell cultures compared with WT cell cultures, suggesting that SMYD3 depletion and Foxp3 inhibition may preferentially permit IL-17 production by $CD4^+$ T cells (**Figure 6b**). To determine the transcriptional level of other TH17-associated genes, mRNA from $SMYD3^{-/-}$ and WT iTreg-skewed cells was assessed. Our results show that besides *il17a*, SMYD3 abrogation also led to the enhancement of *rorc*, *il23r*, *il21*, and *il22* transcripts in

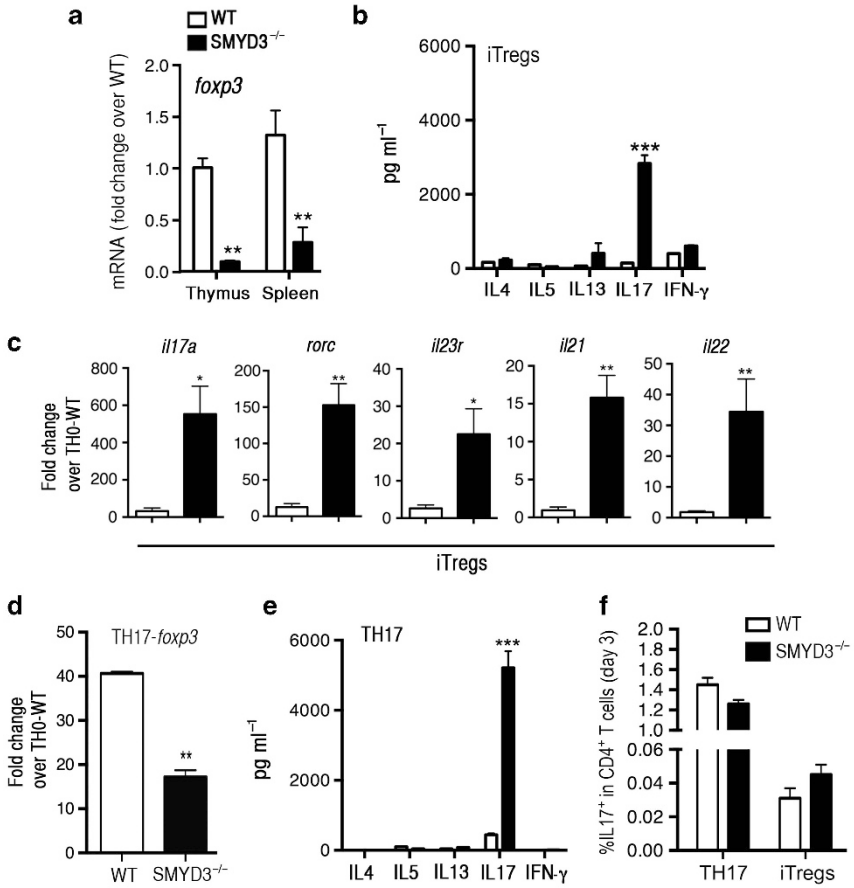

Figure 6 SMYD3 depleted CD4$^+$ T cells are poised to produce the proinflammatory cytokine IL-17. (**a**) Expression levels of *foxp3* mRNA in CD4$^+$ T cells derived from the thymus and spleens of WT and SMYD3$^{-/-}$ mice. (**b**) Naïve CD4$^+$ T cells derived from WT and SMYD3$^{-/-}$ were skewed into inducible regulatory T (iTreg) for 3 days and analyzed for cytokines. (**c**) WT and SMYD3$^{-/-}$-derived iTreg cells were examined for *il17a*, *rorc*, *il23r*, *il21*, and *il22* mRNA by quantitative real-time PCR (q-RT-PCR). Naïve CD4$^+$ T cells derived from WT and SMYD3$^{-/-}$ were skewed into TH17 for 3 days and analyzed for (**d**) *foxp3* mRNA expression and (**e**) cytokine production. (**f**) IL-17 expression was accessed by flow cytometry in WT and SMYD3$^{-/-}$-differentiated TH17 and iTreg cells. Data show mean ± s.e.m. of triplicate wells and are representative of three independent experiments performed with $n = 3$ per group. *$P < 0.05$, **$P < 0.01$, and ***$P < 0.001$.

iTreg-skewing cells (**Figure 6c**). Furthermore, as TH17-skewed cultures also use TGFβ and upregulate *foxp3* gene expression, our studies examined those cultures. Our data demonstrate that even in TH17 cultures SMYD3 appears to regulate *foxp3* expression (**Figure 6d**) and the generation of IL-17-associated phenotype (**Figure 6e**). To investigate whether SMYD3 was impacting the TH17/iTreg lineage decision or influencing cell function, WT and SMYD3$^{-/-}$-naïve CD4+ T cells were differentiated into iTreg cells and TH17 cell cultures, and intracellular IL-17 was measured by flow cytometry to access whether the increase in IL-17 production observed in the SMYD3-deficient cells was due to increased IL-17 production/cell and/or an increase in the frequency of IL-17-producing cells. Our results show similar frequency of IL-17-producing cells in either iTreg cells or TH17 cell cultures, suggesting that the increased IL-17 production observed in the supernatants of SMYD3-deficient cells represents increased IL-17 per cell as opposed to more cells differentiating. Collectively, these data suggest that SMYD3 is important for the regulation of Foxp3 leading to the subsequent regulation of IL-17 production by CD4$^+$ T cells.

SMYD3 deficiency leads to exacerbation of RSV-induced pathology

Given that Treg cells contribute to the control of immune responses against respiratory pathogens, and previous studies related IL-17 with the exacerbation of pulmonary tissue damage and mucus production,[21,22] we examined the effect of SMYD3 deficiency in lung pathology using a mouse model of respiratory syncytial virus (RSV) infection. RSV-infected animals showed upregulation of *foxp3* expression at 2 days postinfection (d.p.i.) (**Figure 7a**), as described previously.[23] SMYD3$^{-/-}$ and WT mice infected with RSV showed that the frequency of CD4$^+$CD25$^+$Foxp3$^+$ Treg cells found in SMYD3$^{-/-}$ mice was significantly lower compared with WT mice even though the total number of Foxp3$^+$ CD4 T cells were not reduced (**Figure 7b**). Infiltration of lymphocytic populations in the lungs showed that activated CD4$^+$CD69$^+$ T cells (**Figure 7c**)

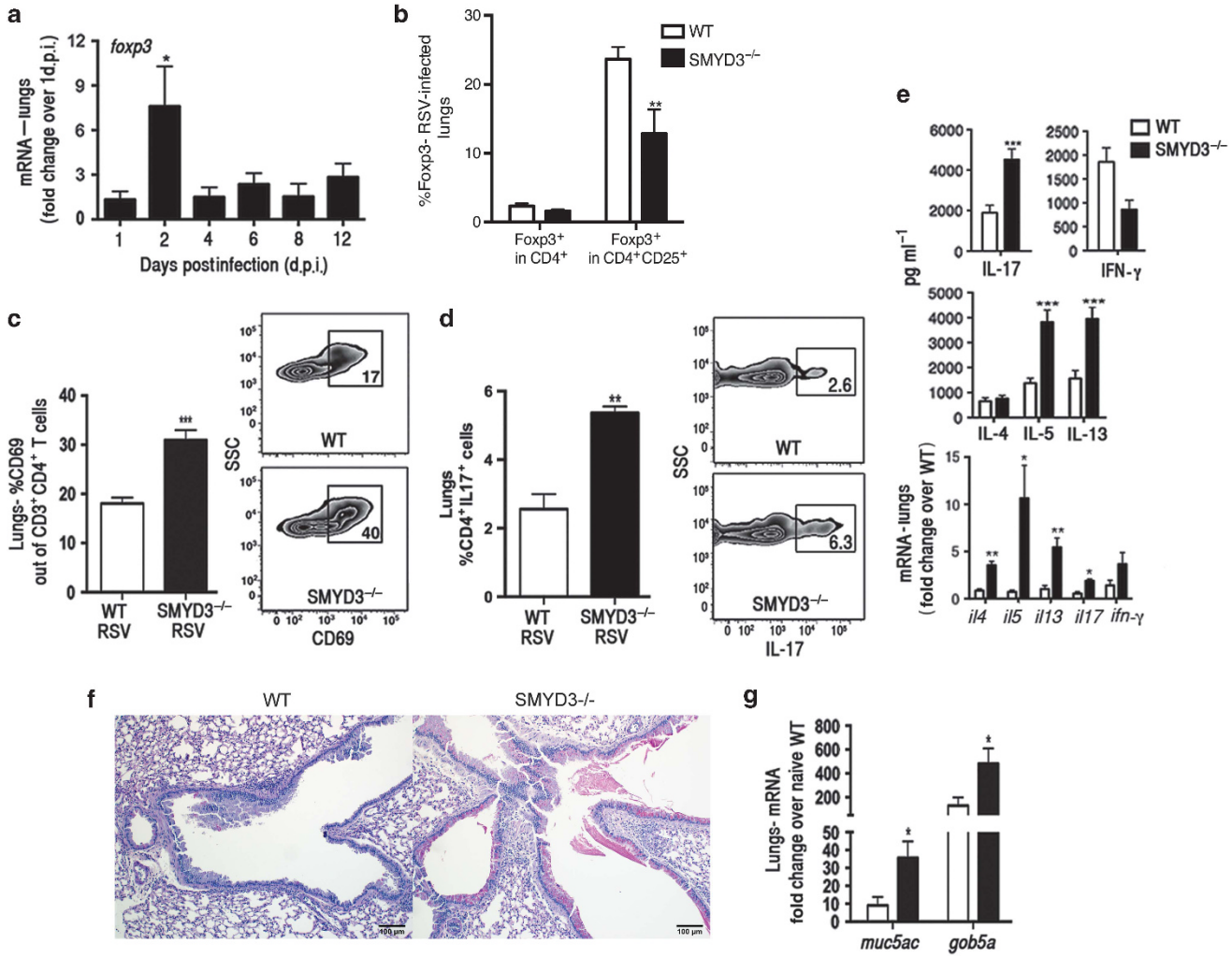

Figure 7 SMYD3 is required to mount a protective immune response against respiratory syncytial virus (RSV) infection. (**a**) C57BL/6 wild-type (WT) mice were infected RSV and lungs were assessed for *foxp3* expression at 1, 2, 4, 6, 8, and 12 ($n=3$) days postinfection (d.p.i.). WT ($n=4$) and SMYD3$^{-/-}$ ($n=4$) were infected with RSV and assessed at 8 d.p.i. (**b**) Percentage of Foxp3^{+} in gated CD3^{+}CD4^{+}CD25^{+} T cells, (**c**) percentage of activated CD69^{+} in gated CD3^{+}CD4^{+} T cells, and (**d**) percentage of CD4^{+}IL-17^{+} TH17 cells in gated CD3^{+} T cells. (**e**) Lungs from RSV-infected WT and SMYD3$^{-/-}$ mice were homogenized, mRNA was extracted, and expression of cytokine was assessed by quantitative real-time PCR (q-RT-PCR). (**f**) Periodic acid-Schiff (PAS) staining of lung sections of WT (left panel) and SMYD3$^{-/-}$ mice (right panel) infected with RSV at 8 d.p.i. (**g**) *Muc5ac* and *gob5a* mRNA in the lungs of RSV-infected WT and SMYD3$^{-/-}$ mice. Data show mean ± s.e.m. of triplicate wells and are representative of three independent experiments. *$P<0.05$, **$P<0.01$, and ***$P<0.001$. SSC, side scatter.

and percentage of TH17 cells (CD4^{+}IL-17^{+}) (**Figure 7d**) infiltrating the lungs of SMYD3$^{-/-}$ mice was significantly higher compared with WT mice. Supernatants from single-cell suspensions of lung-associated lymph nodes (LNs) isolated from RSV-infected SMYD3$^{-/-}$ mice restimulated *ex vivo* with RSV showed enhanced production of IL-17, as well as IL-5 and IL-13 (**Figure 7e**), cytokines known to contribute to lung pathogenesis and airway mucus production during RSV infection.[21,24,25] Cytokine expression studied in lung homogenates of RSV-infected SMYD3$^{-/-}$ mice also showed enhanced cytokine responses similar to the restimulated LNs (**Figure 7e**). Owing to the effect of SMYD3 ablation in the expression of TH2-associated cytokines in the lungs of RSV-infected mice, additional experiments performed *in vitro* explored the effect of SMYD3 in TH2 differentiation. Results showed that SMYD3 depletion leads to enhancement in the production of IL-4 by TH2-differentiating cells (data not shown), suggesting that this molecule may also regulate TH2-associated cytokine production. Histopathological analysis of periodic acid-Schiff-stained lung sections showed enhanced goblet cell hyperplasia and increased mucus secretion in the large airways of SMYD3$^{-/-}$ mice compared with WT mice (**Figure 7f**) as well as increased expression of the mucus-associated genes *muc5ac* and *gob5a* (**Figure 7g**). Thus, during virus-induced respiratory infection, SMYD3 deficiency led to decreased Treg cell infiltration and dysregulated immune responses with increased IL-5, IL-13, and IL-17 production that exacerbated pathology in the lungs.

DISCUSSION

The regulation of the immune response by Treg cells has been examined in nearly every disease response scenario and found to be central in controlling the outcome of immunity and disease severity while demonstrating a tumor-promoting role in cancer.[12,14,26,27] The central determinant of Treg cell development is Foxp3 expression that is constitutively expressed in thymus-derived nTreg cells and transcriptionally regulated by NFAT (nuclear factor of activated T cells), and AP1 in iTreg cells.[13,28–30] Also important in the generation of iTreg cells is the accompanying activation of the TGFβ/Smad3 signaling pathway[15] that correlates with alteration of the CNS1 element at the *foxp3* locus, and that has a functional effect on Foxp3 expression.[16–18] It has been reported that Treg cells can lose their Foxp3 expression in an inflammatory environment and acquire the ability to produce proinflammatory cytokines.[20,31] Elucidating distinct mechanisms that impact Foxp3 expression and defining pathways that can contribute to the stability of Treg cell lineage remain topics of ongoing research. The differentiation of T cells is linked to epigenetic changes in chromatin structure.[31] Previous studies examining T-cell regulation have primarily defined key components that regulate H3K4 (an activating mark) and H3K27 (an inhibitory mark) trimethylation.[32–34] However, the specific epigenetic enzymes that control gene expression in iTreg cells have not been elucidated. In the present studies, a focus on H3K4 regulation was pursued owing to the identification of SMYD3 expression early during the iTreg-skewing process. The maintained expression of SMYD3 was dependent on sustained stimulation with TGFβ that corresponded to the expression of Foxp3 and SMYD3 when the cytokine stimulus was removed.

Importantly, lower expression of SMYD3 was observed in freshly isolated nTreg cells and along with data from siRNA knockdown that indicate no alteration in Foxp3 suggest that SMYD3 is not critical in nTreg cells. These data also correlate with previous studies indicating greater stability of nTreg cell commitment to the $Foxp3^+$ phenotype, whereas iTreg cells may have greater plasticity to be redirected toward other phenotypes and necessitate the presence of TGFβ for maintenance of SMYD3 and stability of Foxp3.[31,35,36] Recent studies indicate that nTreg cells are more potent *in vitro* in T-cell proliferation assays compared with iTreg cells, and further that nTreg cells were more stable in *in vivo* transfer studies allowing protection from inflammatory bowel disease in $Rag2^{-/-}$ mice.[37] The latter study further demonstrated that nTreg cells also had a characteristic CpG hypomethylation pattern that began in the thymus upon T-cell receptor ligation by self-ligands attributing to their greater stability. Interestingly, a study conducted with CNS elements and their role in the *foxp3* gene showed that CNS2 controls the maintenance of Foxp3 expression in mature Treg cells.[16] In the present study, no alteration in the CNS2 region of the *foxp3* promoter was observed when SMYD3 was depleted. Instead, the regulation of Foxp3 by SMYD3 appears to be associated with the *foxp3* promoter and the TGFβ/Smad3 response element CNS1—sites described to be important for iTreg cell conversion.[16] Importantly, although Foxp3 was significantly inhibited, its expression was not completely abolished upon SMYD3 ablation, suggesting that epigenetic changes mediated by SMYD3 enhance *foxp3* transcription in iTreg cells but is not the only element that regulates *foxp3*. This latter observation is consistent with the function of chromatin-modifying enzymes that regulate gene accessibility and allow enhanced access to transcription factors such as Smad3.

The data from the present study also outline the requirement of Smad3 activation for the expression and function of SMYD3 and consequent Foxp3 regulation, clearly implicating SMYD3 as necessary for iTreg development linked to TGFβ activation. We confirmed the importance of TGFβ-mediated signaling for SMYD3 expression using both Smad3 inhibition and knockdown. TGFβ induces Foxp3 expression in T cells and causes TH to iTreg ell conversion and subsequent expansion through Smad signaling.[38] Although these data do not examine other critical gene targets of SMYD3 in Treg cell development, it does confirm that Foxp3 is a transcriptional target of SMYD3. The data show that SMYD3 ablation inhibits H3K4me3 in the CNS1 and promoter region of the *foxp3* locus. CNS1 has been identified as a TGFβ-sensitive element that contains binding sites for NFAT and Smad3.[16,18] Our results suggest that SMYD3 is recruited to CNS1, trimethylates H3K4, making the *foxp3* locus poised for transcription. The *foxp3* promoter region containing NFAT-AP1 response elements was also affected upon SMYD3 ablation, suggesting that TGFβ/SMYD3-induced chromatin remodeling of CNS1 might affect the accessibility of the upstream *foxp3* promoter. Other epigenetic modifications have been associated with repression of Foxp3 in conventional T cells that is at least partially dependent on PIAS1, a SUMO E3 ligase, which binds to the *foxp3* promoter and recruits DNA methyltransferases that keep the *foxp3* promoter in a methylated and silent state (heterochromatin).[39] Removal of PIAS1 in knockout experiments verified its function for the regulation of Foxp3 and generation of nTreg cells that are derived in the thymus.[39] We have not examined whether reduced PIAS1 expression or function is coordinated with the expression of SMYD3.

Abrogation of Foxp3 or its diminished expression in iTreg cells leads to decreased suppressive capability and to the acquisition of proinflammatory properties including production of cytokines including IL-4, IL-17, and interferon-γ.[20] In this study, SMYD3 inhibition and Foxp3 downregulation in $CD4^+$ T cells led to increased production of IL-17. An intimate link between Treg and TH17 cell programs has been identified previously.[40,41] The increased production of IL-17 by $SMYD3^{-/-}$ $CD4^+$ T cells under iTreg-skewing conditions was also demonstrated by the expression of the TH17-associated genes *il17a*, *rorc*, *il23r*, *il21*, and *il22*. Foxp3 expression reduces TH17 differentiation through the inhibition of retinoid-related orphan receptor-γt function.[41] Given that several transcription factors have been described to be associated with the transcription regulation of Foxp3,[42] T-bet and Gata3 were also investigated and not affected by SMYD3 depletion (data not shown). Together, these results suggest that

the loss of Foxp3 by SMYD3 depleted $CD4^+$ T cells reverse Foxp3-mediated inhibition of retinoid-related orphan receptor-γt, thereby promoting IL-17 production.

iTreg cells are crucial players in immune regulation of the lungs during pulmonary disease.[22,23,43,44] During RSV infection, Treg cells suppress antigen-specific T effector cell responses, contribute to the control of viral replication, and minimize tissue damage.[22,44] Accordingly, RSV-infected SMYD3-deficient mice had lower levels of Treg cells in the lungs and LNs accompanied by increased T-cell responses with greater lung and airway inflammation. Our results also demonstrated that in addition to decreased Treg cells, RSV-infected SMYD3-deficient mice fail to control the T-cell cytokine (IL-5, IL-13, and IL-17) and RSV-associated pathogenic responses, such as airway goblet cell hyperplasia. IL-17 can increase mucus production with consequent exacerbation of tissue damage. These data in virus infection demonstrate that without proper iTreg cell development in $SMYD3^{-/-}$ mice, a dysregulated immune environment develops.

In summary, our studies demonstrate a novel role for SMYD3 as a TGFβ/SMAD3-inducible epigenetic enzyme that has a central role for enhancing Foxp3 expression during immune responses and regulating proinflammatory IL-17 production. Enhancement of lung pathology during pulmonary infection triggered by RSV in mice deficient in SMYD3 lends further support to this notion. Our observations suggest that TGFβ signaling is required for SMYD3 activation, subsequent H3K4 methylation in the *foxp3* loci, and maintenance of Foxp3 expression levels in iTreg cells. Overall, these data highlight SMYD3 as a potential target for manipulating Foxp3 and iTreg cell response during infection, autoimmunity, and cancer.

METHODS

Mice. Female WT C57BL/6 mice (6–10 weeks old) were purchased from Taconic (Hudson, NY). Breeding pairs of Foxp3 eGFP reporter mice ($Foxp3^{eGFP}$, B6.Cg-$Foxp3^{TM2Tch}$/J) were purchased from The Jackson Laboratory, Bar Harbour, ME and bred in-house. CD4-Cre mice were obtained from Taconic. $SMYD3^{tm1a\ (KOMP)\ Wtsi}$ mice in a C57BL/6 background were derived from KOMP Repository at UC Davis (Davis, CA). The allele contains loxP and FRT sites, thus Cre and FLP deletion were used to create an SMYD3 conditional knockout resulting in a null allele in $CD4^+$ cells ($SMYD3^{fl/fl}CD4^{Cre+}$). All mice were housed in the University Laboratory Animal Facility at the University of Michigan Medical School (Ann Arbor, MI). All animal experiments were conducted according to animal protocols approved by The Animal Use Committee at the University of Michigan.

Extracellular and intracellular staining for flow cytometry. Cells were stained using antibodies against surface markers CD3 (145-2C11), CD4 (RM4-5), and CD25 (7D4) (all from eBioscience or BD Biosciences, San Jose, CA), permeabilized, fixed, and labeled for intracellular Foxp3 (FJK-16s), IL-4 (11B11), interferon-γ (IFNγ), and IL-17 (eBio17B7). Samples were acquired on an LSRII flow cytometer (BD Biosciences) with the use of FACSDiva software (BD Biosciences). Data were analyzed using the FlowJo software (TreeStar, FLOWJO, LLC, Ashland, Oregon).

***In vitro* T-cell conversion**. Naïve $CD4^+$ T cells were enriched from the spleens of WT, $SMYD3^{-/-}$, or $Foxp3^{eGFP}$ mice as described.[18] Cells stimulated for 48 h to 5 days using plate-bound anti-CD3 (2.5 μg ml^{-1}; eBioscience), soluble anti-CD28 (3 μg ml^{-1}; eBioscience) plus TGFβ (2–20 ng ml^{-1}), and rIL-2 (10 ng ml^{-1}; all from R&D Systems). Human naïve $CD4^+$ T cells were isolated as above and converted into iTreg cells using 5 ng ml^{-1} of TGFβ. For Thelper (H) cell differentiation, naïve $CD4^+$ T cells were skewed towards TH17 using IL-6 (1 ng ml^{-1}) and TGFβ (2 ng ml^{-1}) plus anti-interferon-γ (10 μg ml^{-1}), anti-IL-12 (10 μg ml^{-1}), anti-IL-4 (10 μg ml^{-1}), and anti-CD28 (3 μg ml^{-1}).

Quantitative RT-PCR. Gene expression levels were determined as described.[45] For PCR arrays, RNA was converted to cDNA and analyzed on a mouse epigenetic chromatin modification enzymes PCR array platform (PAMM-085; SA Biosciences) following the manufacturer's protocol. PCR array results were analyzed using the RT2 Profiler PCR Array Data Analysis (SA Biosciences).

ChIP assay. ChIP assay was performed as described[3] using anti-Smad3 antibody (Ab) (C67H9; Millipore, Billerica, MA), anti-SMYD3 Ab (ab16027; Abcam, Cambridge, MA), anti-H3K4me3 Ab (ab8580), and normal rabbit immunoglobulin G (IgG) as a control. Regions of the Foxp3 promoter, Foxp3 CNS1, -2, and -3, were amplified by SYBR Green qPCR (Applied Biosciences, Valencia, CA) and quantified in triplicates or quadruplicates with the percent of input method. The following primers were used: SMYD3 (forward, 5′-CCCCGTTGCACTCAGACCCC-3′ and reverse, 5′-GGCTGTC CAGACCAGAAGCTCA-3′), Foxp3 promoter (forward, 5′-GGGC ACTCAGCACAAACATGATG-3′ and reverse, 5′-GAGGCTT CCTTCTGCCCAAAC-3′), Foxp3 CNS1 (forward, 5′-GTTTTG TGTTTTAAGTCTTTTGCACTTG-3′ and reverse, 5′-CAGTAAAT GGAAAAAATGAAGCCATA-3′), Foxp3 CNS2 (forward, 5′-GTT GCCGATGAAGCCCAAT-3′ and reverse, 5′-ATCTGGGCCCTGTT GTCACA-3′), and Foxp3 CNS3 (forward, 5′-AATGAATGAGAC ACAGAACTATTAAGATGA-3′ and reverse, 5′-CAGACGGTGCC ACCATGAC-3′).

Cytokine assay. Cytokines from supernatants of *in vitro* culture assays were measured using BioPlex System and Suspension Array Technology (Bio-Rad, Hercules, CA).

Western blot. Western blots were performed using antibodies anti-SMYD3 (Abcam), anti-H3K4me3 (Millipore), anti-SMAD3 (Abcam), anti-Foxp3 (eBioscience), or β-actin (Sigma, St Louis, MO) as control primary antibody; the membrane was counterstained with horseradish peroxidase-conjugated rabbit or mouse IgG antibody and visualized with enhanced chemiluminescence detection reagents (GE Healthcare, Aurora, OH).

siRNA assay. Naïve $CD4^+$ T cells were transfected with 2 μM of Smad3-specific, SMYD3-specific, or nontargeting control siRNAs (Dharmacon, Lafayette, CO) using mouse T-cell Nucleofector Kit (Lonza Walkersville, Allendale, NJ). Transfected cells were kept in mouse T cells nucleofector medium for 18–24 h at 37 °C with 5% CO_2, harvested, and stimulated under TH0 or Treg cell-skewing conditions.

Suppression assay. Splenic $CD4^+CD25^{HI}$ nTreg cells derived from naïve WT and $SMYD3^{-/-}$ mice were stained as before and FACS-sorted. Splenic naïve $CD4^+$ T cells were isolated from WT mice, labeled with 2.5 μM CFSE (Invitrogen, Waltham, MA), and cocultured with nTreg cells derived from WT or $SMYD3^{-/-}$ mice in complete medium with plate-bound anti-CD3 monoclonal Ab (2.5 μg ml^{-1}) and soluble anti-CD28 (3 μg ml^{-1}) (eBiocience) for 3 days. Suppression was analyzed by flow cytometry.

Cell proliferation assay. Naïve $CD4^+$ T cells were labeled with CFSE and incubated under iTreg-skewing conditions for 3 days. Proliferation was analyzed by flow cytometry.

Confocal analysis. Cell suspension from naïve and iTreg-skewing cells stained as described[45] using mouse anti-CD4 (BD Pharmingen, San Jose, CA), rabbit anti-Smyd3 (Abcam), goat anti-rabbit Alexa Fluor 568, and anti-mouse Alexa Fluor 488 (Invitrogen). The stained

tissue sections were analyzed using a Nikon A1 confocal microscope system (Nikon Instruments, Melville, NY).

RSV infection and primary cell isolation from infected mice. The RSV A strain (line 19) was derived from a clinical isolate at the University of Michigan and propagated in HEp-2 cells (ATCC, Manassas, VA). Line 19 elicits disease in mice comparable to severe RSV infection in humans, including significant airway hyperresponsiveness and mucus overproduction.[46] LN cells were cultured (5×10^5 per well in a 96-well plate) and restimulated with RSV (multiplicity of infection = 0.5) for 48 h for RNA and cytokine measurements.

Histology. Organs were perfused with 4% formaldehyde for fixation and embedded in paraffin using standard histological techniques. Lung sections were stained with PAS to detect mucus production. All other tissues were stained with hematoxylin and eosin. Tissue sections were evaluated using light microscopy by an independent blinded observer.

Statistical analysis. Data were analyzed using GraphPad prism software version 6 (GraphPad, San Diego, CA). Measures between two groups were performed with a Student's *t*-test (two-tailed). Groups of three or more were analyzed by one-way analysis of variance followed by Tukey's post-testing and $P<0.05$ was considered significant ($^{*}P<0.05$, $^{**}P<0.01$, and $^{***}P<0.001$).

SUPPLEMENTARY MATERIAL is linked to the online version of the paper at http://www.nature.com/mi

ACKNOWLEDGMENTS

We thank Susan Morris, Andrew Rasky, Ron Allen, Ana L. Coelho, Amrita D. Joshi, Lisa Riggs Johnson, and Pamela Lincoln for technical assistance; Robin Kunkel for art work; and Dr onnett for critical reading of the manuscript. This work was supported by the NIH grants: AI073876 (to N.W.L.) and T32 AI007413 (to D.D.A.N.).

DISCLOSURE

The authors declared no conflict of interest.

REFERENCES

1. Dawson, M.A. & Kouzarides, T Cancer epigenetics: from mechanism to therapy. *Cell* **150**, 12–27 (2012).
2. Ehrensberger, A.H. & Svejstrup, J.Q Reprogramming chromatin. *Crit. Rev. Biochem. Mol. Biol.* **47**, 464–482 (2012).
3. Wen, H., Dou, Y., Hogaboam, C.M. & Kunkel, S.L Epigenetic regulation of dendritic cell-derived interleukin-12 facilitates immunosuppression after a severe innate immune response. *Blood* **111**, 1797–1804 (2008).
4. Wilson, C.B., Rowell, E. & Sekimata, M Epigenetic control of T-helper-cell differentiation. *Nat. Rev. Immunol.* **9**, 91–105 (2009).
5. Ruden, D.M. & Lu, X Hsp90 affecting chromatin remodeling might explain transgenerational epigenetic inheritance in *Drosophila*. *Curr. Genom.* **9**, 500–508 (2008).
6. Hamamoto, R. *et al.* SMYD3 encodes a histone methyltransferase involved in the proliferation of cancer cells. *Nat. Cell Biol.* **6**, 731–740 (2004).
7. Tsuge, M. *et al.* A variable number of tandem repeats polymorphism in an E2F-1 binding element in the 5' flanking region of SMYD3 is a risk factor for human cancers. *Nat. Genet.* **37**, 1104–1107 (2005).
8. Frank, B. *et al.* Variable number of tandem repeats polymorphism in the SMYD3 promoter region and the risk of familial breast cancer. *Int. J. Cancer* **118**, 2917–2918 (2006).
9. Cock-Rada, A.M. *et al.* SMYD3 promotes cancer invasion by epigenetic upregulation of the metalloproteinase MMP-9. *Cancer Res.* **72**, 810–820 (2012).
10. Kanno, Y., Vahedi, G., Hirahara, K., Singleton, K. & O'Shea, J.J Transcriptional and epigenetic control of T helper cell specification: molecular mechanisms underlying commitment and plasticity. *Annu. Rev. Immunol.* **30**, 707–731 (2012).
11. Locksley, R.M Nine lives: plasticity among T helper cell subsets. *J. Exp. Med.* **206**, 1643–1646 (2009).
12. Ziegler, S.F FOXP3: of mice and men. *Annu. Rev. Immunol.* **24**, 209–226 (2006).
13. Li, Q. *et al.* Constitutive nuclear localization of NFAT in Foxp3+ regulatory T cells independent of calcineurin activity. *J. Immunol.* **188**, 4268–4277 (2012).
14. Shevach, E.M., DiPaolo, R.A., Andersson, J., Zhao, D.M., Stephens, G.L. & Thornton, A.M The lifestyle of naturally occurring CD4+ CD25+ Foxp3+ regulatory T cells. *Immunol. Rev.* **212**, 60–73 (2006).
15. Floess, S. *et al.* Epigenetic control of the foxp3 locus in regulatory T cells. *PLoS Biol.* **5**, e38 (2007).
16. Zheng, Y., Josefowicz, S., Chaudhry, A., Peng, X.P., Forbush, K. & Rudensky, A.Y Role of conserved non-coding DNA elements in the Foxp3 gene in regulatory T-cell fate. *Nature* **463**, 808–812 (2010).
17. Tone, Y., Furuuchi, K., Kojima, Y., Tykocinski, M.L., Greene, M.I. & Tone, M Smad3 and NFAT cooperate to induce Foxp3 expression through its enhancer. *Nat. Immunol.* **9**, 194–202 (2008).
18. van der Veeken, J., Arvey, A. & Rudensky, A Transcriptional control of regulatory T-cell differentiation. *Cold Spring Harbor Symp. Quant. Biol.* **78**, 215–222 (2013).
19. Kitani, A., Fuss, I., Nakamura, K., Kumaki, F., Usui, T. & Strober, W Transforming growth factor (TGF)-beta1-producing regulatory T cells induce Smad-mediated interleukin 10 secretion that facilitates coordinated immunoregulatory activity and amelioration of TGF-beta1-mediated fibrosis. *J. Exp. Med.* **198**, 1179–1188 (2003).
20. Williams, L.M. & Rudensky, A.Y Maintenance of the Foxp3-dependent developmental program in mature regulatory T cells requires continued expression of Foxp3. *Nat. Immunol.* **8**, 277–284 (2007).
21. Mukherjee, S. *et al.* IL-17-induced pulmonary pathogenesis during respiratory viral infection and exacerbation of allergic disease. *Am. J. Pathol.* **179**, 248–258 (2011).
22. Lund, J.M., Hsing, L., Pham, T.T. & Rudensky, A.Y Coordination of early protective immunity to viral infection by regulatory T cells. *Science* **320**, 1220–1224 (2008).
23. Fulton, R.B., Meyerholz, D.K. & Varga, S.M Foxp3+ CD4 regulatory T cells limit pulmonary immunopathology by modulating the CD8 T cell response during respiratory syncytial virus infection. *J. Immunol.* **185**, 2382–2392 (2010).
24. Lotz, M.T. & Peebles, R.S Jr Mechanisms of respiratory syncytial virus modulation of airway immune responses. *Curr. Allergy Asthma Rep.* **12**, 380–387 (2012).
25. Durant, L.R., Makris, S., Voorburg, C.M., Loebbermann, J., Johansson, C. & Openshaw, P.J Regulatory T cells prevent Th2 immune responses and pulmonary eosinophilia during respiratory syncytial virus infection in mice. *J. Virol.* **87**, 10946–10954 (2013).
26. Ziegler, S.F. & Buckner, J.H Influence of FOXP3 on CD4+CD25+ regulatory T cells. *Expert Rev. Clin. Immunol.* **2**, 639–647 (2006).
27. Bos, P.D., Plitas, G., Rudra, D., Lee, S.Y. & Rudensky, A.Y Transient regulatory T cell ablation deters oncogene-driven breast cancer and enhances radiotherapy. *J. Exp. Med.* **210**, 2435–2466 (2013).
28. Wu, Y. *et al.* FOXP3 controls regulatory T cell function through cooperation with NFAT. *Cell* **126**, 375–387 (2006).
29. Lee, S.M., Gao, B. & Fang, D FoxP3 maintains Treg unresponsiveness by selectively inhibiting the promoter DNA-binding activity of AP-1. *Blood* **111**, 3599–3606 (2008).
30. Samstein, R.M. *et al.* Foxp3 exploits a pre-existent enhancer landscape for regulatory T cell lineage specification. *Cell* **151**, 153–166 (2012).
31. Zhou, X., Bailey-Bucktrout, S., Jeker, L.T. & Bluestone, J.A Plasticity of CD4(+) FoxP3(+) T cells. *Curr. Opin. Immunol.* **21**, 281–285 (2009).
32. Lal, G. & Bromberg, J.S Epigenetic mechanisms of regulation of Foxp3 expression. *Blood* **114**, 3727–3735 (2009).
33. Koyanagi, M., Baguet, A., Martens, J., Margueron, R., Jenuwein, T. & Bix, M EZH2 and histone 3 trimethyl lysine 27 associated with Il4 and Il13 gene silencing in Th1 cells. *J. Biol. Chem.* **280**, 31470–31477 (2005).

34. Yamashita, M. *et al.* Crucial role of MLL for the maintenance of memory T helper type 2 cell responses. *Immunity* **24**, 611–622 (2006).
35. Zhou, X. *et al.* Cutting edge: all-*trans* retinoic acid sustains the stability and function of natural regulatory T cells in an inflammatory milieu. *J. Immunol.* **185**, 2675–2679 (2010).
36. Murai, M., Krause, P., Cheroutre, H. & Kronenberg, M Regulatory T-cell stability and plasticity in mucosal and systemic immune systems. *Mucos. Immunol.* **3**, 443–449 (2010).
37. Ohkura, N. *et al.* T cell receptor stimulation-induced epigenetic changes and Foxp3 expression are independent and complementary events required for Treg cell development. *Immunity* **37**, 785–799 (2012).
38. Fantini, M.C., Becker, C., Monteleone, G., Pallone, F., Galle, P.R. & Neurath, M.F Cutting edge: TGF-beta induces a regulatory phenotype in CD4 + CD25 − T cells through Foxp3 induction and down-regulation of Smad7. *J. Immunol.* **172**, 5149–5153 (2004).
39. Liu, B., Tahk, S., Yee, K.M., Fan, G. & Shuai, K The ligase PIAS1 restricts natural regulatory T cell differentiation by epigenetic repression. *Science* **330**, 521–525 (2010).
40. Bettelli, E. *et al.* Reciprocal developmental pathways for the generation of pathogenic effector TH17 and regulatory T cells. *Nature* **441**, 235–238 (2006).
41. Zhou, L. *et al.* TGF-beta-induced Foxp3 inhibits T(H)17 cell differentiation by antagonizing RORgammat function. *Nature* **453**, 236–240 (2008).
42. Rudra, D. *et al.* Transcription factor Foxp3 and its protein partners form a complex regulatory network. *Nat. Immunol.* **13**, 1010–1019 (2012).
43. Curotto de Lafaille, M.A., Kutchukhidze, N., Shen, S., Ding, Y., Yee, H. & Lafaille, J.J Adaptive Foxp3 + regulatory T cell-dependent and -independent control of allergic inflammation. *Immunity* **29**, 114–126 (2008).
44. Loebbermann, J. *et al.* Regulatory T cells expressing granzyme B play a critical role in controlling lung inflammation during acute viral infection. *Mucos. Immunol.* **5**, 161–172 (2012).
45. Kittan, N.A. *et al.* Cytokine induced phenotypic and epigenetic signatures are key to establishing specific macrophage phenotypes. *PLoS One* **8**, e78045 (2013).
46. Huber, S. *et al.* Th17 cells express interleukin-10 receptor and are controlled by Foxp3(−) and Foxp3 + regulatory CD4 + T cells in an interleukin-10-dependent manner. *Immunity* **34**, 554–565 (2011).